Kinetics of fatigue crack growth and crack paths in the old puddled steel after 100-years operating time

G. Lesiuk, M. Szata
Wroclaw University of Technology, Faculty of Mechanical Engineering, Department of Mechanics, Materials Science and Engineering, Smoluchowskiego 25, PL-50-370 Wroclaw, Poland
Grzegorz.Lesiuk@pwr.edu.pl, Mieczyslaw.Szata@pwr.edu.pl

ABSTRACT. The goal of the authors' investigations was determination of the fatigue crack growth in fragments of steel structures (of the puddled steel) and its cyclic behavior. Tested steel elements coming from the turn of the 19th and 20th were gained from still operating ancient steel construction (a main hall of Railway Station, bridges etc.). This work is a part of investigations devoted to the phenomenon of microstructural degradation and its potential influence on their strength properties. The analysis of the obtained results indicated that those long operating steels subject to microstructure degradation processes consisting mainly in precipitation of carbides and nitrides inside ferrite grains, precipitation of carbides at ferrite grain boundaries and degeneration of pearlite areas [1, 2]. It is worth noticing that resistance of the puddled steel to fatigue crack propagation in the normalized state was higher. The authors proposed the new kinetic equation of fatigue crack growth rate in such a steel. Thus the relationship between the kinetics of degradation processes and the fatigue crack growth rate also have been shown. It is also confirmed by the materials research of the viaduct from 1885, which has not shown any significant changes in microstructure. The non-classical kinetic fatigue fracture diagrams (KFFD) based on deformation ($\Delta\delta$) or energy (ΔW) approach was also considered. In conjunction with the results of low- and high-cycle fatigue and gradual loss of ductility as a consequence (due to the microstructural degradation processes) - it seems to be a promising construction of the new kinetics fatigue fracture diagrams with the energy approach.

KEYWORDS. Puddled steel; Kinetic fatigue fracture diagram; Mechanical degradation.

INTRODUCTION

The rapid development of metallurgy in the 19th century resulted in intensive erection of numerous bridges. Many of them are still operating. Operation of the advanced in age technical objects becomes a common phenomenon in the current reality. The problem becomes particularly acute in bridge sector. It can be estimated from the works [3] and [4], that the age of 68% of railroad bridges exceeds 50 years, while 28% of them are over 100 years old objects. The maintenance of such aged objects in full usefulness and reliability requires adequate diagnostic methods and evaluation of their reliability. It should be prepared independently from the procedures adopted in normative regulations

for the modern technical objects. In case of objects erected at the turn of the 19th and 20th centuries, the diversification of operating conditions, as well as the peculiar characteristics of materials used for their building require individualized approach in the assessment of their condition. This fact is associated with insufficient knowledge of the material properties – the puddled and mild (rimmed) steel. Also, the presence of degradation processes makes impossible adaptation of material data from the literature. Typical macro- and microstructure vies have been shown in Fig. 1.

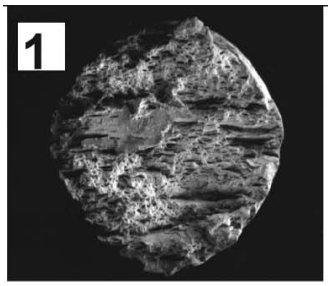

Specimen after tension test (puddled iron produced in 1890).

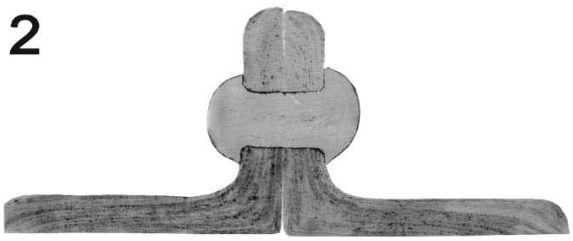

Sulphurous print (puddled iron produced in Germany in 1882)

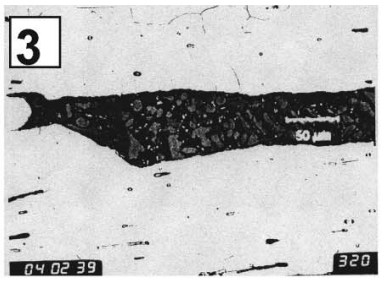

Microscan with large slags (some mm) in layered structure.

Figure 1: Characteristics of puddled iron [5].

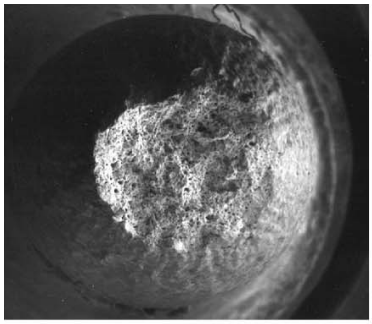

Specimen after tension test (rimmed steel, produced in 1900).

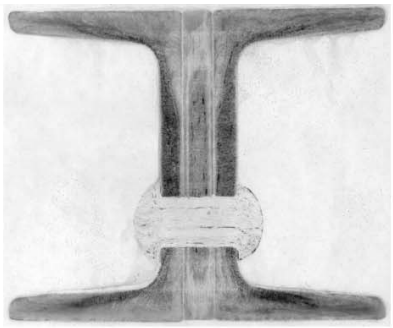

Sulphurous print (rimmed steel, produced in 1900).

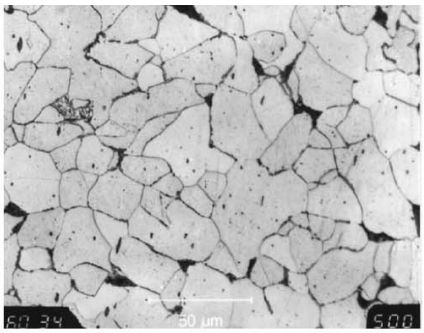

Micro-scan with large diameter of grain (~ 50 µm).

Figure 2: Characteristics of early mild iron (rimmed steel), [5]

The difference in the structure of these steels is significant. Their macroscopic structure and the manufacturing process are essential for the strength properties - what emphasizes the obtained results. From the historical point of view, it can be assumed that by the end of the 19th century the puddled steel was commonly operating. At the beginning of the 20th century it was completely displaced by the mild rimmed steel.

These low-carbon steels (typically less than 0.1% C) tend to degradation processes and brittleness. From the application point of view, it is necessary to determine the safe life of the construction or the structural components from puddled/mild rimmed steel. In order to evaluate the sub-critical period of fatigue crack growth - it is necessary to know the material constants responsible for kinetic of fatigue crack growth rate (i.e. Paris law constants C and m). In this case, despite the similar chemical compositions, for such a type of steel – mainly puddled – the range and variability of mentioned constants is relatively large. The problem of cracks in the puddled steels is particularly important due to their common location in the joints - steel pieces were joined using riveting as a dominant technique. After 100-hundred operating time, the cracks caused by fatigue and corrosion existed. In conjunction with the microstructural degradation processes (precipitation of carbides and nitrides inside ferrite grains, precipitation of carbides at ferrite grain boundaries and degeneration of pearlite areas) such combination can be especially dangerous.

MATERIAL EXAMINATION

For the material examination the structural components were gained from old historic building and viaducts. Three types of beams were examined; B (steel beam I220, 1855-1857) and S (steel beam, 1899-1904) – coming from the 19th century Main Railway Station in Wroclaw, and W – steel (flat bar from balustrade, 1885 year) – is gained from

historic viaduct. The chemical composition has been obtained due to the gravimetric method. The results are included in Tab. 1.

chemical element [%, wt]	B-steel	S-steel	W-steel	typical puddled steel, [5]
C	0.03	0.06	0.08	0.03-0.15
Mn	0.06	0.1	0.25	0.054-0.11
Si	0.03	0.17	0.15	0.03-0.42
P	0.028	0.198	0.245	0.011-0.39
S	0.045	0.025	0.015	0.034-0.018

Table 1: Chemical composition of the investigated material

The chemical compositions of tested materials suggest that they belong to a group of the puddled steel. The results of metallographic observation (Fig. 3-4) confirm this fact. For the puddled steels, the high phosphorus content is very characteristic.

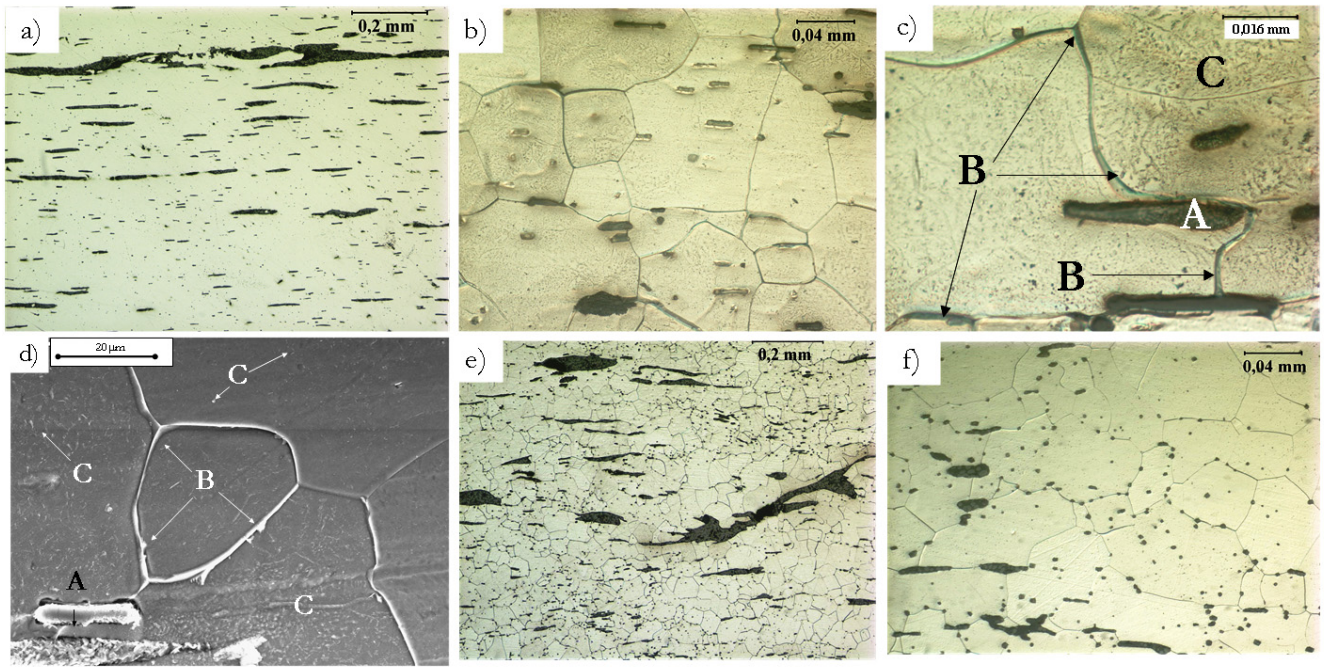

Figure 3: Microstructure of investigated puddled steel (1899-1904) – marked as B and W -steel, in (a) post-operating state (light microscopy) – presented nonmetallic inclusions typical for puddled steel, (b) post-operating state; ferrite grains with numbers of nonmetal inclusions, (c) magnified ferrite grains structure with nonmetallic inclusions – mainly silicates (A) and thick envelope of Fe_3C_{III} on the grain boundary (B) with numbers of degradation separations brittle phase inside ferrite grains (C), post-operating state SEM, etched 3%HNO_3, (d) magnified ferrite grains with degradation symptoms; thick enveloper of Fe_3C_{III} (B) and separations inside ferrite grain (C), post-operating state SEM, etched 3%HNO_3, (e) the microstructure of the W-steel in post-operating state, high numbers of deformed nonmetallic inclusions – an area of the extreme presence of the non-metallic inclusions, etched 3%HNO_3, (f) typical ferrite grains structure of the W – steel, based on [2]

Static tensile test results and impact resistance examination

The basic mechanical properties of delivered steel are collected in Tab. 2. A significant change in the impact strength has been noted. The yield tensile stress and ultimate tensile stress are not always coincident with a level of microstructural degradation processes. It is postulated that the measure of degradation should be the impact strength as a basic (qualitative) measure in engineering practice.

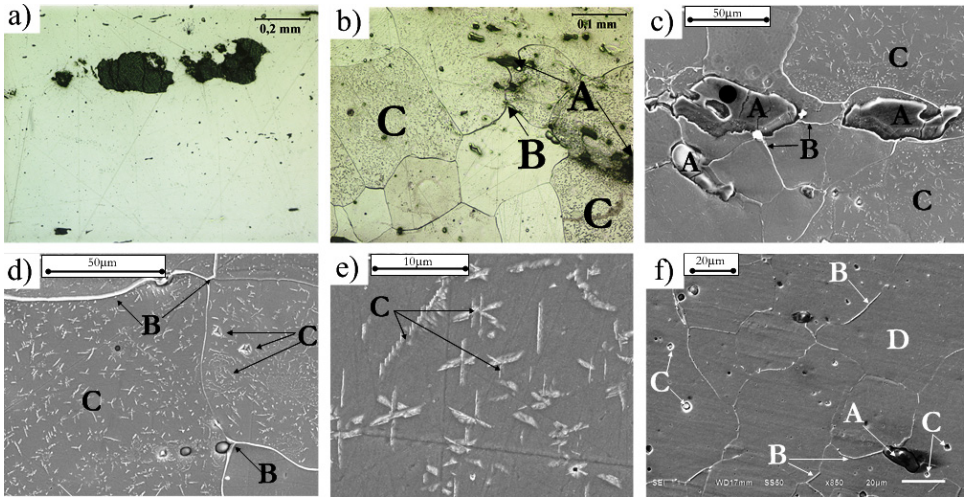

Figure 4: Microstructure of investigated puddled steel (1899-1904) – marked as S-steel, in (a) post-operating state (light microscopy) – presented nonmetallic inclusions typical for puddled steel, (b) post-operating state; ferrite grains with numbers of nonmetal inclusions (A) and degradation separations (C) inside ferrite grains and also thick envelope Fe_3C_{III} on the grain boundary (light microscopy, etched 3%HNO_3), (c) ferrite grains structure with nonmetallic inclusions – mainly silicates (A) and thick envelope of Fe_3C_{III} on the grain boundary (B) with numbers of degradation separations brittle phase inside ferrite grains (C), post-operating state SEM, etched 3%HNO_3, (d) magnified ferrite grains with degradation symptoms; thick enveloper of Fe_3C_{III} (B) and separations inside ferrite grain (C), post-operating state SEM, etched 3%HNO_3, (e) magnified area of ferrite grain with brittle separations (C), post-operating state SEM, etched 3%HNO_3, (f) microstructure of ferrite grains with nonmetal inclusion (A) (after normalisation) with significantly reduced number of degradation symptoms; (B) – remains of the brittle separations on the grain boundary, (C) – minor amounts of separations inside ferrite grain, SEM, etched 3%HNO_3, [2], [6].

	B-steel [P/N]	S-steel [P/N]	W-steel [P/N]	Typical values for puddled steel, [5]
YTS [MPa]	264.8/257.4	257.6/242	263/294	220-280
UTS [MPa]	372.8/379.5	376/340	359.7/368.6	330-400
Elongation at break A [%]	20.8/24.9	20.8/22.7	15.1/27.1	8-25
Necking Z [%]	28.2/27	34/36.8	33.9/39	variable
Impact resistance test results, Charpy value [J/cm^2]	35/49	37/58	n/a	variable

Table 2: Strength properties of the investigated materials in post-operating state (P) and after heat treatment – normalising (N).

FATIGUE PROPERTIES

Low-cycle tests results

A low cycle fatigue test for the puddled steel (S-steel) – 5 round specimen ϕ12 mm for each test step, controlled total strain amplitude $\Delta\varepsilon_t$=0.2%, 0.25%, 0.3%, 0.35%, 0.4%, f=0.2Hz – was performed with accordance to the standards ASTM E606. The stabilized hysteresis loops were selected for analysis, corresponding to half of the number of cycles to destruction. The graphs of fatigue life of specimens in the after-operation and normalized states are presented in Fig. 5. These curves are known in the literature as Coffin and Manson equation:

$$\frac{\Delta\varepsilon_t}{2} = \varepsilon'_f \left(2N_f\right)^c + \frac{\sigma'_f}{E}\left(2N_f\right)^b, \tag{1}$$

where:

$\Delta\varepsilon_t/2$ – total strain amplitude,
ε_f' - fatigue ductility coeficients,
σ_f' – cyclic fatigue strength coeficient in MPa,
$2N_f$ – number of reversals to failure,
c – fatigue ductility exponent,
b – fatigue strength exponent.

For the puddled steel in the post-operating steel ε_f'=0.0169, σ_f'=442 MPa, and exponents c=-0.3632 and b=-0.03651. For steel after heat treatment, these parameters were following; ε_f=0.01626, σ_f=378 MPa, c=-0.3165, b=-0.02702. The obtained results show much worse cyclical properties of the puddled steel in the after-operating state in comparison to the normalized state. The significant change with the transition number of cycled $2N_t$ (marked dashed line in Fig. 5). The typical hysteresis loops ($\Delta\varepsilon$=0.4%) for as-received state (P) and after normalisation state (N) have been shown in Fig. 6. It can be noted the higher ductility of the material for the normalized state. The yield point in the first cycles of the loading is noticeable (Fig. 6b). It is probably caused by the presence of degradation processes.

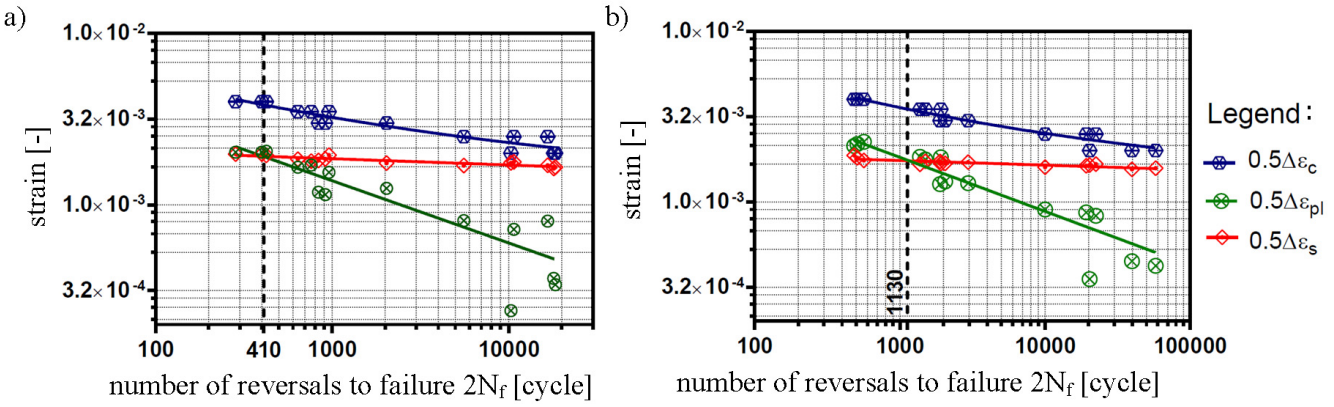

Figure 5: (a) Coffin-Manson curve for puddled steel in post-operating state, (b) Coffin-Manson curve for puddled steel in normalized state for puddled steel [6].

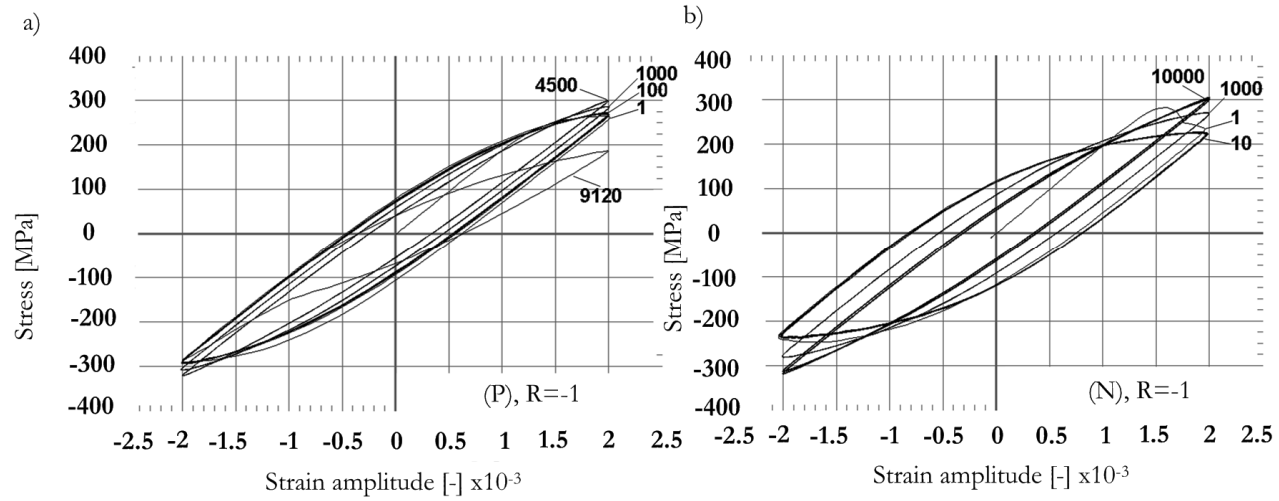

Figure 6: Hysteresis loops ($\Delta\varepsilon$=0.4%), a) for as-received state (P) and b) after normalization state (N).

FATIGUE CRACK GROWTH RATE AND ANALYTICAL DESCRIPTION

In order to obtain the kinetic fatigue fracture diagram (KFFD), the CT specimens were tested (in accordance with the American Standard ASTME 647). The characteristic dimensions of the specimen are following; W = 48 mm and thickness t = 10-15 mm, a/W=0.275. The fatigue crack length was measured with the compliance variation method

and it was periodically corrected *via* moving microscope (with camera). The stress ratio R=0.1 was kept and testing frequency was established on the level 12.5 Hz. During the experiment, the force, displacement and crack opening displacement (COD) signals were registered. Two types of diagrams were constructed –on the bases of magnitude of the stress intensity factor ΔK and (according to the [7]) $\Delta\delta_t$ – CTOD (crack tip opening displacement). The method for estimating the value of CTOD has been described in the work [7]. The CTOD was obtained by the formula:

$$\Delta\delta_t = \frac{\Delta K^2}{E\sigma_y}. \tag{2}$$

Fatigue crack growth rate model for puddled steel

From the experimental results it can be concluded that the most sensitive markers of degradation are the impact resistance toughness and low cycle fatigue properties. The relationship between impact resistance toughness and fatigue crack growth conditions with the structural degradation nature of puddled steels was demonstrated below by the following equation proposed by the authors:

$$\frac{da}{dN} = \frac{A}{KCV^3\sigma_{pl}^2}\sqrt{\left(\frac{KCV_{35}}{E}\right)^3}\left(\Delta K^5 - \Delta K_{th}^5\right) \tag{3}$$

In the proposed model: A means non-dimensional constant (A=2457 for post-operating state, A=1871 for normalized state), KCV means the impact energy value (Charpy test value) in J/cm², KCV_{35} - required minimal energy value (35 J/cm²) for the modern steel, E represents Young modulus in MPa, σ_{pl} – yield tensile strength in MPa.

In several studies (i.e. [7, 8, 9]), the relationship between low-cycle fatigue properties and the kinetics of fatigue crack growth in metals has been proposed. The base of consideration is always the dissipated energy during the cyclic loading. According to Ramberg-Osgood equation and Coffin-Manson (1), the specific energy till fracture has been proposed in the work [9] as:

$$Wc = 4\sigma'_f\varepsilon'_f - \frac{4n'}{1+n'}\left(\frac{\sigma'_f}{k'}\right)^{1/n'}\cdot\sigma'_f \tag{4}$$

$$Wc = \frac{4}{1+n'}\sigma'_f\varepsilon'_f \tag{5}$$

where:

Wc – specific energy till fracture in J/m³,

n' – cyclic strain hardening exponent,

k' – cyclic strength coefficient in MPa.

According to the works [9, 10, 11, 12], the tensor components of the stress and the strain can be described as follows (under a small scale yielding assumption, HRR [10] singularity crack tip field):

$$\Delta\sigma_{ij} = \Delta\sigma'_y\left(\frac{\Delta K_I^2}{\alpha'\Delta\sigma'^2_y I_{n'}r}\right)^{n'/(1+n')}\cdot\tilde{\sigma}_{ij}(\theta;n') \tag{6}$$

$$\Delta\varepsilon^p_{ij} = \frac{\alpha'\sigma'_y}{E}\left(\frac{\Delta K_I^2}{\alpha'\Delta\sigma'^2_y I_{n'}r}\right)^{1/(1+n')}\cdot\tilde{\varepsilon}_{ij}(\theta;n'), \tag{7}$$

where:

$\tilde{\sigma}_{ij}(\theta;n')$ - non-dimensional angular distribution functions of HRR stress singularities,

$\tilde{\varepsilon}_{ij}(\theta;n')$ - non-dimensional angular distribution functions of HRR strain singularities,

σ_y' – cyclic yield stress in MPa, ($\Delta\sigma_y' \approx 2\,\sigma_y'$),

I_n' – non-dimensional exponent of n',

ρ - radial coordinate ahead of a crack tip,

θ - angular coordinate ahead of a crack tip.

The cyclic plastic zone (for mode I loading) with Huber-Mises-Hencky (HMH) yielding criterion for a plane stress can be expressed (according to the [9, 10, 11, 12]) as:

$$\Delta\rho(\theta)=\frac{\Delta K_I^2}{8\pi(1+n')\Delta\sigma_y'^{\,2}}\left(1+\frac{3}{2}\sin^2\theta+\cos\theta\right) \tag{8}$$

In this case, the total plastic energy dissipated in a cyclic plastic zone ϕ_p (according to [9]) can be expressed as:

$$\phi_p=\frac{A_1\Delta K_I^2}{8\pi(1+n')\Delta\sigma_y'^{\,2}EI_{n'}}\left(\frac{1-n'}{1+n'}\right) \tag{9}$$

where:

$$A_1=\int_0^{2\pi}\left(1+\frac{3}{2}\sin^2\theta+\cos\theta\right)\tilde{\sigma}_{eq}(\theta,n')\tilde{\varepsilon}_{eq}(\theta,n')d\theta. \tag{10}$$

Fatigue crack will grow if the specific energy values ϕ_p' (the specific fracture energy referred to the unit of area (J/m) is reached. The authors [9] have been described the fatigue crack growth rate as:

$$\frac{da}{dN}=\frac{\phi_p'}{Wc}, \tag{11}$$

using the formula (1) or (2) [9] we can obtain:

$$\frac{da}{dN}=\frac{A_1(1-n')}{7\pi I_{n'}E\sigma_f'\varepsilon_f'}\left(K_{\max}-K_{th}\right)^2. \tag{12}$$

In addition to the cyclical properties, the critical value of the stress intensity factor K_{fc} and its variability (degradation) depending on the degree of microstructural degradation processes should be also considered. In the literature, K_{fc} is often replaced by a critical stress intensity factor K_c (for mode I loading). Therefore, after reduction and assumption that:

$$\alpha=f\left(I_n',A_1,const\right), \tag{13}$$

a new kinetic equation of fatigue crack growth rate for puddled steel is proposed:

$$\frac{da}{dN}=\frac{\alpha(1-n')}{E\sigma_f'\varepsilon_f'}\left(\Delta K-\Delta K_{th}\right)^2\cdot\left(1+\frac{\Delta K}{K_c-K_{\max}}\right)^4. \tag{14}$$

The fracture toughness of investigated S-steel was estimated using J-integral as a critical value of fracture toughness K_c converted from J-integral using formula:

$$K_I = \sqrt{\frac{E \cdot J_I}{\left(1-\nu^2\right)}} \quad . \tag{15}$$

For investigated steel, K_c was estimated at the level of K_c=134,4 MPa√m for as-received state, and for normalized state, fracture toughness is close to K_c=147 MPa√m. Based on experimental results, the constant α was estimated at the level of α = 3. The different values of the α for the post-operating and normalized states is postulated. This fact can be explained by the dependence (10) on the A_1 value, so the plastic deformation ahead of the crack tip. In connection with microstructural degradation processes and dislocation motion blocking system, the lower plastic deformation ahead of the crack tip in the post-operating state (in accordance with the results of the LCF) should be expected. The assumption (13) needs further investigation for different type of the puddled steel, on the other hand, the experimental dependence provides the constant value α. The experimental data for S – steel in post-operating and normalized states with the prediction in the near-threshold regime fitting using model (3) and (14) have been presented in Fig. 7.

For the steels B and W the experimental data were not so comprehensive – particularly in low-cycle fatigue investigation. Therefore, in case of B and W steels, the fatigue fracture diagrams have been constructed using a method described in [7], where the force, deformation and energy approach have been discussed. All the results with exponent model data fitting are shown in Fig. 8. It is noted, that for the puddled steel the typical experimental data scatter. The differences in the kinetics of fatigue fracture are most reflected in the near-threshold regime. It should be underlined that the fatigue crack growth rate curves for W-steel are prepared just from 3 specimens – due to the material limitations.

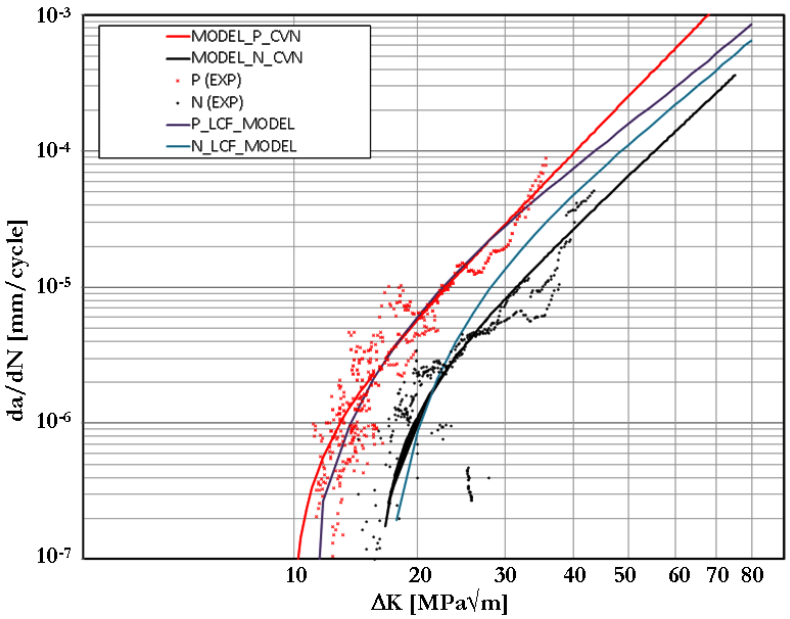

Figure 7: Fatigue crack growth rate for puddled steel (S) in post-operating state and normalized state, experimental data with proposed models fitting.

CONCLUSIONS

The paper presents the investigation results of microstructural and mechanical properties for an old steel from the 19th century. All tested materials were identified for the puddled steel – commonly used at the turn of the 19th and 20th century. In all materials, the microstructural degradation processes were also identified. These processes mainly consist in precipitation of carbides and nitrides inside ferrite grains, precipitation of carbides at ferrite grain boundaries and degeneration of pearlite areas. The most sensitive parameters (in terms of microstructural degradation processes) estimated in simply engineering test is the impact resistance value. The degradation processes progress can be

also identified during the tensile static tests in changes of elongation and reduction in area in normalized state. The yield stress does not always correspond to the structural changes.
For the S-steel, the complex low-cycle fatigue and fatigue crack growth resistance tests were performed. The results indicate the worsening of the cyclic properties and fatigue crack growth in accordance with the degradation processes level. According to the [2] and [9], the authors have proposed a new kinetic equation for description of fatigue crack growth rate for the puddled steel. Due to the low-material data consumption, the model (3) can explain the differences in fatigue fracture. The proposed new model (14) needs the complex data for cyclic properties. In this case, it seems that the degradation model (14) behavior (Fig. 7) is close to the experimental results. According to the [7], the kinetic fatigue fracture diagrams for B and W steels have been constructed. The differences in the fatigue crack growth rate have been identified. In comparison to the force approach and ΔK basis in fatigue fracture diagrams, the CTOD is more sensitive for degradation changes in kinetics of fatigue crack growth in the puddled steel. In the light of the experimental results and deliberations in the works [7-9], it seems that energy description for the fatigue crack growth rate and microstructural degradation influence is a promising approach.

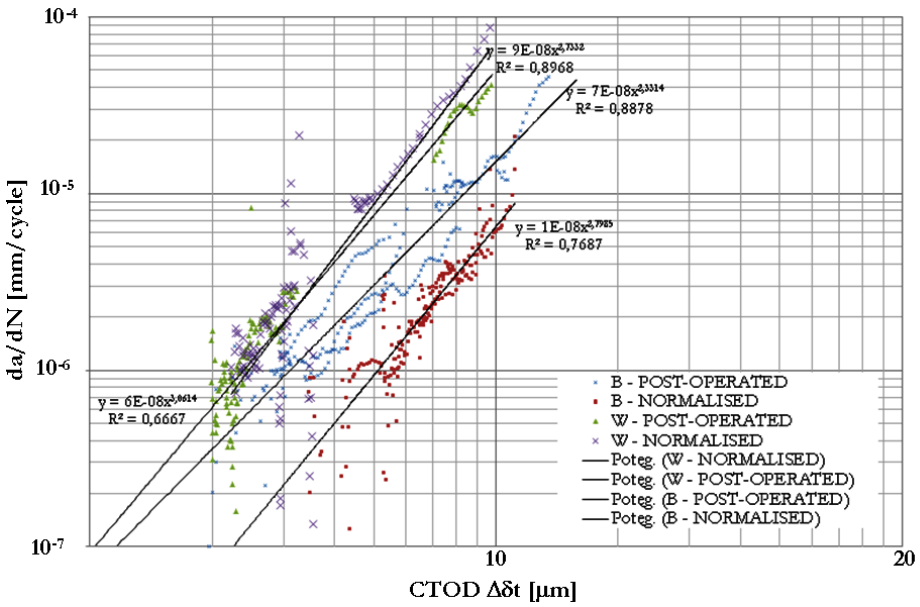

Figure 8: Kinetic fatigue fracture diagram for steel B and W.

ACKNOWLEDGMENTS

This work has been supported in part by the project B40075/PWR/W10/K10.

REFERENCES

[1] Lesiuk, G., Szata, M., Aspects of structural degradation in steels of old bridges by means of fatigue crack propagation, Materials Science (New York), 47 (1) (2011) 82-88.
[2] Lesiuk, G., Mechanical and structural degradation of 19th puddled steel, Wroclaw University of Technology, PhD Thesis, (2013), in Polish.
[3] Bień, J., Damage to bridges and diagnostics, Wydawnictwo Komunikacji i Łączności, Warszawa, (2010), in Polish.
[4] Björklund, A., Höglind, J., Strengthening of steel structures with bonded prestressed laminates. Master thesis, Department of Structural Engineering, Chalmers University of Technology, (2007) 1-8.
[5] Helmerich, R., Kühn, B., Nussbaumer, A., Assessment of existing steel structures. A guideline for estimation of the remaining fatigue life, Structure and Infrastructure Engineering, 3(3) (2007) 245 – 255.

[6] Lesiuk, G., Szata, M., Fatigue properties and fatigue crack growth in puddled steel with consideration of microstructural degradation processes after 100-years operating time, XVII International Colloquium on Mechanical Fatigue of Metals (ICMFM17), Procedia Engineering, 74 (2014) 64–67. DOI:10.1016/j.proeng.2014.06.225.
[7] Ostash, O.P., Panasyuk, V.V., Andreiko, I.M., Chepil', R.V., Kulyk, V.V., Vira, V.V., Methods for the construction of the diagrams of fatigue crack-growth rate of materials, Materials Science, 43(4) (2007).
[8] Szata, M., Modeling of fatigue crack growth using energy method, Publishing House of Wroclaw University of Technology, Poland, Wroclaw, (2002), in Polish.
[9] Pandey, K. N., Chand, S., Fatigue crack growth model for constant amplitude loading, Fatigue Fracture Eng. Mat. Structures, 27 (2004) 459-472.
[10] Hutchinson, J.W., Singular behaviour at the end of a tensile crack in a hardening material. J. Mech. Phys. Solids, 16 (1968) 13–31.
[11] Izumi, Y., Fine, M. E., Mura, T., Energy consideration in fatigue crack propagation. Int. J. Fract. 17 (1981) 15–25.
[12] Ellyin, F., Fatigue damage, crack growth and life prediction, Chapman & Hall, (1997).